Thermodynamic properties and entropy scaling law for diffusivity in soft spheres

S. Pieprzyk,[1,*] D. M. Heyes,[2,†] and A. C. Brańka[1,‡]

[1]*Institute of Molecular Physics, Polish Academy of Sciences, Mariana Smoluchowskiego 17, 60-179 Poznań, Poland*

[2]*Department of Physics, Royal Holloway, University of London, Egham, Surrey TW20 0EX, United Kingdom*

(Received 30 April 2014; published 3 July 2014)

The purely repulsive soft-sphere system, where the interaction potential is inversely proportional to the pair separation raised to the power n, is considered. The Laplace transform technique is used to derive its thermodynamic properties in terms of the potential energy and its density derivative obtained from molecular dynamics simulations. The derived expressions provide an analytic framework with which to explore soft-sphere thermodynamics across the whole softness-density fluid domain. The trends in the isochoric and isobaric heat capacity, thermal expansion coefficient, isothermal and adiabatic bulk moduli, Grüneisen parameter, isothermal pressure, and the Joule-Thomson coefficient as a function of fluid density and potential softness are described using these formulas supplemented by the simulation-derived equation of state. At low densities a minimum in the isobaric heat capacity with density is found, which is a new feature for a purely repulsive pair interaction. The hard-sphere and $n = 3$ limits are obtained, and the low density limit specified analytically for any n is discussed. The softness dependence of calculated quantities indicates freezing criteria based on features of the radial distribution function or derived functions of it are not expected to be universal. A new and accurate formula linking the self-diffusion coefficient to the excess entropy for the entire fluid softness-density domain is proposed, which incorporates the kinetic theory solution for the low density limit and an entropy-dependent function in an exponential form. The thermodynamic properties (or their derivatives), structural quantities, and diffusion coefficient indicate that three regions specified by a convex, concave, and intermediate density dependence can be expected as a function of n, with a narrow transition region within the range $5 < n < 8$.

DOI: 10.1103/PhysRevE.90.012106 PACS number(s): 65.20.De, 05.20.−y, 65.40.gd

I. INTRODUCTION

There are a number of simple model pair potentials for molecules in the fluid state which have proved useful in testing statistical mechanical approaches (e.g., perturbation or integral liquid methods with different closures) and whose physical properties elucidate the behavior of more complex molecular fluids. Examples include the hard-sphere fluid and the Lennard-Jones particle system. This work is concerned with the physical properties of another key model system, which is composed of particles interacting through the repulsive soft-sphere or inverse power (IP) potential,

$$\phi(r) = \epsilon\left(\frac{\sigma}{r}\right)^n, \tag{1}$$

where r is the separation between two particles, σ is the particle diameter, ϵ sets the energy scale, and n is a parameter determining the potential hardness (the potential softness, $s = n^{-1}$).

This potential form is significant because many nanoscale particles have a soft repulsive core which can be represented by a soft sphere and used as a reference system in classical perturbation theories of liquids [1,2]. For steeply repulsive spheres, $n \gg 1$, and the model provides an alternative route to the properties of hard-sphere (HS) systems, being the limiting case when $n \to \infty$ [3–5]. The softer (small n) systems have been used in studies of the crystal-solid interface [6] and some liquid metal properties [7,8]. A soft potential of simple analytic form can be used to establish the generic consequences of softness on the physical properties of particle assemblies. A wide spectrum of practically important systems from the very soft to the extremely hard can be modeled by varying, s. The softness of a particle, for example, is an important characteristic in soft matter research, in particular for colloidal and polymeric particulate systems such as small polymerically stabilized colloids, star polymers, dendrimers, emulsions, and microgels. Indeed, for microgel particles this potential form has been used to interpret experimentally measured physical properties [9,10]. In some cases, the particles interpenetrate much more than in simple molecular fluids, and the consequences of this for the physical properties are still not well understood, despite many mean-field statistical mechanical and computer simulation treatments [11–13]. Although effective interparticle interactions have been derived for many of the different classes of colloidal and polymeric systems, they are of variable analytic form [14–16], and it is useful to consider a generic soft potential that is not linked to any specific class of particle, to bring out wider ranging issues and trends.

The self-similar IP potential, possesses some useful (even unique) properties, in that, for example, excess thermodynamic properties do not depend on the density and temperature separately but on a dimensionless combination of the two, a temperature-scaled density $\tilde{\rho} = (\beta\epsilon)^{\frac{3}{n}}\rho\sigma^3$ or the corresponding packing fraction $\zeta = \pi\tilde{\rho}/6$, where $\rho = N/V$ is the number density, N is the number of particles in volume V, and $\beta = 1/k_BT$ with k_B Boltzmann's constant and T the temperature [17]. Therefore, for a given n, the entire phase behavior or T-ρ plane can be mapped out by performing computations along a single isotherm or isochore. Furthermore, several basic

*pieprzyk@ifmpan.poznan.pl
†david.heyes@rhul.ac.uk
‡branka@ifmpan.poznan.pl

physical properties of a system of IP particles are related to each other, e.g., pressure and mechanical properties are directly related to the interaction energy per particle [18]. Thus, for any n, a common theoretical treatment for the static properties can be made, which is not possible for other potentials, such as the Lennard-Jones form.

The HS limit and intermediate n values (particularly $n = 12$) have been studied many times in the literature (e.g., see [17,19–22]). More recently, the present authors and co-workers have explored the pressure and n dependence of the transport coefficients [23,24] and their particle force distribution functions [25,26]. General features of the radial distribution functions and their asymptotic behavior have also been explored [27].

The solid-fluid phase boundary as a function of n has been determined [28,29] and the virial coefficients of soft-sphere fluid been calculated up to the eighth for a range of n [30,31].

The IP scaling properties were found by Roland, Bair, and Casalini [32] to be useful in collapsing experimental viscosity data onto master curves using, in effect, the IP scaling parameter, $(T/T_R)(V/V_R)^\gamma$, where T_R and V_R are the temperature and molar volume, respectively, of a reference system. The exponent γ is exactly $n/3$ for an IP fluid but is used as a fit parameter in treating the experimental data; the value of γ varies for different classes of molecule to reflect their different effective softnesses. This density-temperature scaling procedure [33] was subsequently applied to superpose self-diffusion coefficients for Lennard-Jones liquids [34] and relaxation and liquid crystal thermodynamic data [35]. In addition, Dyre and co-workers, [36–41] developed the concept of "strongly correlating" or Roskilde fluids, which are liquids where the equilibrium virial-potential energy correlation coefficient is at least 0.9 (this number is always 1 for IP liquids, which therefore acts as a benchmark fluid). This approach allows invariant trends in structural, static, and dynamical properties to be mapped out, and helps to explain the origins of empirical correlations between these quantities for real or model systems found in the past [42,43]. Shell has shown that this scaling follows from a statistical mechanical coarse graining procedure [44].

The practical usefulness of the IP system relies on having direct access to properties of the system at any point in the density-softness plane. This work gives new details of the physical properties of the soft-sphere system in the density-softness plane. The main focus is on the thermodynamic properties and a relationship between entropy and diffusion coefficient. The study is limited to the softness range $n > 3$, as for $n \leqslant 3$ this potential does not lead to a thermodynamically stable system because the volume integral of the potential diverges.

The expressions for thermodynamic properties of the soft-sphere system in the density-softness plane are derived and analyzed in Sec. II. In Sec. III details of the molecular dynamics (MD) simulations are presented. The behavior of all the main thermodynamic properties are discussed in Sec. IV along, with analysis of the softness dependence of structural properties and related freezing criteria. In Sec. V a relationship between the self-diffusion coefficient and the excess entropy for the soft-sphere fluid is discussed. Conclusions are presented in Sec. VI.

II. THE LTT METHOD AND SOFT SPHERES

In a series of publications by Lustig [45] and then Meier and Kabelac [46] it was shown that all thermodynamic variables can be expressed in terms of phase-space quantities, Ω_{mn}, which are functions of MD ensemble averages of the kinetic energy, the inverse kinetic energy, the volume derivatives of the potential energy, and combinations of these. Their treatment is a generalization of a Laplace transform technique (LTT), introduced by Pearson, Halicioglu, and Tiller [47] for the derivation of the exact thermodynamic expressions in the microcanonical ensemble. Recently, the LTT method has been used to obtain the thermodynamic properties of a Gaussian core model fluid [48], water [49], and supercritical $n-m$ Lennard-Jones fluids [50]. Explicit expressions for some of the low index Ω_{mn} are [46]

$$\Omega_{00} = \frac{2\langle K\rangle}{3N-3}, \tag{2}$$

$$\Omega_{01} = \frac{N-1}{V}k_BT - \left\langle \frac{\partial U}{\partial V}\right\rangle, \tag{3}$$

$$\Omega_{11} = \frac{N-1}{V} + \left[1 - \frac{3N-3}{2}\right]\left\langle K^{-1}\frac{\partial U}{\partial V}\right\rangle, \tag{4}$$

$$\Omega_{20} = -\left[1 - \frac{3N-3}{2}\right]\langle K^{-1}\rangle, \tag{5}$$

and

$$\Omega_{02} = \frac{2}{3V}\frac{N-2}{V}\langle K\rangle - \left[1 - \frac{3N-3}{2}\right]\left\langle K^{-1}\left(\frac{\partial U}{\partial V}\right)^2\right\rangle - \left\langle \frac{\partial^2 U}{\partial V^2}\right\rangle - 2\frac{N-1}{V}\left\langle \frac{\partial U}{\partial V}\right\rangle, \tag{6}$$

where $\langle\cdots\rangle$ denotes an ensemble or time average in the *NVE***PG** ensemble, which maintains both constant total momentum (**P**) and a quantity (**G**) which is related to the initial position of the center of mass. The total energy, E, is the sum of the kinetic, K, and potential, U, energy terms. Knowing Ω_{00}, Ω_{01}, Ω_{11}, Ω_{02}, and Ω_{20}, several important thermodynamic quantities can be obtained, such as temperature, $T = (\partial E/\partial S)_V$, pressure, $P = T(\partial S/\partial V)_E$, isochoric heat capacity, $C_V = [(\partial^2 S/\partial E^2)_V]^{-1}$, isothermal pressure coefficient, $\gamma_V = (\partial P/\partial T)_V$, and the isothermal bulk modulus, $B_T = -V(\partial P/\partial V)_T$,

$$T = \Omega_{00}/k_B, \quad P = \Omega_{01}, \tag{7}$$

$$C_V = k_B(1 - \Omega_{00}\Omega_{20})^{-1}, \tag{8}$$

$$\gamma_V = \frac{k_B(\Omega_{11} - \Omega_{01}\Omega_{20})}{1 - \Omega_{00}\Omega_{20}}, \tag{9}$$

$$B_T = \frac{V\left[\Omega_{01}(2\Omega_{11} - \Omega_{01}\Omega_{20}) - \Omega_{00}\Omega_{11}^2\right]}{1 - \Omega_{00}\Omega_{20}} - V\Omega_{02}. \tag{10}$$

Using these quantities, the remaining thermodynamic properties can be expressed as a combination of the Ω

TABLE I. The thermodynamic properties of the soft-sphere system in terms of $\langle U \rangle$ and its density derivative derived within the LTT, where $J = \frac{N-1}{N}$ and $Z' = \frac{\partial Z}{\partial \zeta}$.

Z	Compressibility factor	$Z = \frac{P}{\rho k_B T} - J = \frac{n}{3}\frac{\langle U \rangle}{N k_B T} = \frac{n}{3}u$
C_V	Isochoric heat capacity	$\frac{C_V}{N k_B} = \frac{3}{2}J - \zeta \frac{9}{n^2}Z' + \frac{3}{n}Z$
C_P	Isobaric heat capacity	$\frac{C_P}{N k_B} = \frac{3}{2}J - \zeta \frac{9}{n^2}Z' + \frac{3}{n}Z + \frac{(J - \zeta \frac{3}{n}Z' + Z)^2}{J + \zeta Z' + Z}$
B_T	Isothermal bulk modulus	$\frac{B_T}{\rho k_B T} = J + \zeta Z' + Z$
B_S	Adiabatic bulk modulus	$\frac{B_S}{\rho k_B T} = J + \zeta Z' + Z + \frac{(J - \zeta \frac{3}{n}Z' + Z)^2}{\frac{3}{2}J - \zeta \frac{9}{n^2}Z' + \frac{3}{n}Z}$
B_V	Volume expansion	$T B_V = \frac{J - \zeta \frac{3}{n}Z' + Z}{J + \zeta Z' + Z}$
γ_V	Isothermal pressure coefficient	$\frac{T\gamma_V}{\rho k_B T} = J - \zeta \frac{3}{n}Z' + Z$
γ_G	Grüneisen parameter	$\gamma_G = \frac{J - \zeta \frac{3}{n}Z' + Z}{\frac{3}{2}J - \zeta \frac{9}{n^2}Z' + \frac{3}{n}Z}$
μ_{JT}	Joule-Thompson coefficient	$\mu_{JT} = \frac{-\frac{1}{\rho k_B}(\frac{3}{n}+1)Z'\zeta}{\frac{5}{2}J^2 + (\frac{3}{2} - \frac{6}{n} - \frac{9}{n^2})JZ'\zeta + (\frac{7}{2} + \frac{3}{n})JZ - (\frac{3}{n} + \frac{9}{n^2})ZZ'\zeta + (\frac{3}{n}+1)Z^2}$

functions in accordance with the thermodynamic relations given in Ref. [51]. These include the adiabatic bulk modulus $B_S = -V(\partial P/\partial V)_S = B_T + NT\gamma_V{}^2/\rho C_V$, the isobaric heat capacity $C_P = (\partial H/\partial T)_P = C_V B_S/B_T$, the volume expansivity $B_V = (\partial V/\partial T)_P/V = \gamma_V/B_T$, the Joule-Thomson coefficient $\mu_{JT} = (\partial T/\partial P)_H = V(T\gamma_V/B_T - 1)/C_P$, and the Grüneisen parameter $\gamma_G = V(\partial P/\partial E)_V = V\gamma_V/C_V$, where $H = E + PV$ is the enthalpy.

Therefore, a complete thermodynamic description of an equilibrium system can potentially be obtained within the LTT treatment from several MD averages. The main difficulty in using the alternative route fluctuation expressions (e.g., see Chapter 6.2 in Ref. [51]) is that the calculated thermodynamic property is less accurate than that obtained by the LTT because it is obtained from the average of the small difference between large numbers. Also, to improve the accuracy a long simulation with a large number of particles is required as the relaxation time for the fluctuations is longer than for average itself. The Ω functions shown above, apart from $\langle K \rangle$, require five different averages. Typically, for certain potential forms some of these averages, such as $\langle K^{-1} \rangle$ or $\langle (\partial U/\partial V)^2/K \rangle$, are not obtained with sufficient accuracy to allow full exploration of the LTT scheme. The unique features of the IP system allow a considerable reduction in the number of averages which are required. Furthermore, in this case, as shown in the Appendix, a complete thermodynamic description may be obtained from the equation of state and its first derivative only. From MD, Z is obtained directly, and Z' is obtained from these Z values. The derived expressions in Table I provide a practical and reliable means to obtain the thermodynamic properties of the soft-sphere system.

From the derived expressions and taking into account the thermodynamic stability conditions $C_V > 0$ and $B_T > 0$, several general conclusions can already be made. For example, from the form of C_V it follows that $Z - \frac{3}{n}\zeta Z' \geqslant 0$ in the IP system. Consequently, for any (n,ζ), then $(Z + J)(1 + 3/n) \geqslant T\gamma_V/\rho k_B T \geqslant 1$, where J is defined in the caption of Table I. Also because Z' is positive, which follows from the fact that $n\langle U \rangle/3Nk_B$ is an increasing function of ζ in the IP system, we have $B_T \geqslant T\gamma_V$. This implies that the Joule-Thomson coefficient is always nonpositive $\mu_{JT}(\zeta,n) \leqslant 0$ and the volume expansivity is not greater than $1/T$ or $1 \geqslant TB_V(\zeta,n) > 0$.

Some limiting cases of the expressions in Table I can be readily derived. For the HS or $n \to \infty$ limit all terms containing $3/n$ and $9/n^2$ are negligible and can be eliminated, which gives directly the following thermodynamic properties of the HS system, $C_V/Nk_B = 3/2$, $C_P/Nk_B = 3/2 + \rho k_B T(1 + Z)^2/B_T$, $T\gamma_V/\rho k_B T = 1 + Z$, $B_S = B_T + 2\rho k_B T(1 + Z)^2/3$, $\gamma_G = 2(1 + Z)/3$, $TB_V = (1 + Z)/(1 + Z + \zeta Z')$, and $\mu_{JT}k_B = -\pi Z'/(15 + 9Z'\zeta + 21Z + 6Z^2)$. Some of these expressions appear to be new, or at least not presented in the literature in this form, for example, those for C_P and μ_{JT}. Exploiting the analytic equation of state (EoS) for the HS fluid (e.g., [52], or that proposed by Kolafa and given in Ref. [53]) it can be shown that, apart from the constant C_V and monotonically decreasing B_V, all of the thermodynamic expressions considered here are monotonically increasing functions of density for the HS fluid.

The low density limit is also of interest, as some explicit analytic expressions can be derived in this case using the virial series representation of the EoS, $Z(n,\zeta) = \Sigma B_{i+1}\zeta^i$. The number of currently known virial coefficients, $B_i(n)$, of the IP system varies with n, from more than ten in the case of the HS fluid up to eight for certain n values for the soft-sphere case [30,31]. The second virial coefficient is known for all soft-sphere systems and is $B_2 = 4\Gamma(1 - 3/n)$, where $\Gamma(x)$ denotes the gamma function. The radius of convergence of the virial series is not determined, but a comparison with simulation data for many different model systems has shown that it can represent well the low density region. As some of the lower order virial coefficients of the softer soft-sphere systems are negative, in those cases, only the very low density region can reliably be approximated by the first few terms of the virial series (resummation of the virial series for the soft-sphere fluids is more difficult than for the HS fluid [30,31]). The simplest low density approximation of the thermodynamic expressions is that in which Z is represented by $B_2\zeta$ only. This yields, for example, $\gamma_G(\zeta \to 0) = 2/3 + 2\zeta B_2(1 - 3/n)(1 - 2/n)/3$ and shows that the initial slope of $\gamma_G(\zeta)$ decreases with softness from $8/3$ for the HS to the limiting value $8/9$ for $n \to 3$. It may also be seen that the isochoric heat capacity increases with the softness and $T\gamma_V/\rho k_B T(n,\zeta \to 0) = 1 + B_2(1 - 3/n)\zeta$. For given ζ the last quantity has a minimum at $n \approx 5.57$ and the

same maximum value for the most soft ($n \to 3$) and most hard ($n \to \infty$) IP fluids. In addition, with this approximation, the isobaric heat capacity is

$$\frac{C_P}{Nk_B}(Z = B_2\zeta) \equiv C_P^0 = \frac{2.5 + \zeta B_2\left[3 + \left(1 - \frac{3}{n}\right)\left(2 + \frac{3}{n}\right)\right] + \zeta^2 B_2{}^2\left(1 - \frac{9}{n^2}\right)}{1 + 2B_2\zeta}. \tag{11}$$

The extremum condition, $\partial C_P^0/\partial\zeta = 0$, yields $2B_2^2(1 - 3/n)\zeta^2 + 2B_2(1 - 3/n) - 3/n = 0$, which has one physical solution, $\zeta_{\min}(n) = [(\{n+3\}/\{n-3\})^{1/2} - 1]/2B_2$. Thus, this lowest order representation of Z reveals the existence of a minimum in $C_P(n,\zeta)$ which has not been noted before. Also, any soft-sphere fluid is expected to have such a minimum at a particular low density. For the HS fluid $\zeta_{\min}(1/n = 0) = 0$ and $C_P^0(1/n = 0, \zeta_{\min}) = 2.5$ and it can be shown that in this case this minimum is also the solution of the extremum condition, $\partial C_P/\partial\zeta(1/n = 0, \zeta) = 0$. Thus, in the limiting case of the HS system the isobaric heat capacity, $C_P(1/n = 0, \zeta)$, is an increasing function from its minimum value at $\zeta = 0$. To obtain the opposite limit of extremely soft spheres, $\zeta_{\min}$ is first expressed in the equivalent form $[(1 - 9/n^2)^{1/2} - (1 - 3/n)]/8(1 - 3/n)\Gamma(1 - 3/n)$, where the property of the Γ function, $\lim_{x\to 0} x\Gamma(x) = 1$ has been used. This expression gives, $\zeta_{\min}(n \to 3) \to 0$, which means that also in the limit of very soft-sphere fluids the position of the C_P^0 minimum shifts towards zero density, where the minimum value is 1.5. Thus, for very soft spheres, C_P^0 in the range $0 < \zeta < \zeta_{\min}$ is a strongly decreasing function, from 2.5 to the value $C_P^0(n, \zeta_{\min}) > 1.5$ at $\zeta_{\min}$. In the limit $n \to 3$, C_P^0 jumps from 2.5 to 1.5 at $\zeta = 0$. The main features of C_P obtained within the lowest density approximation in Eq. (11) have been confirmed in simulations of the soft-sphere systems which are presented in Sec. III.

It is stressed that the minimum in C_P in fluids is a relatively new observation. The first evidence for the existence of such a minimum was made only recently by Sadus and co-workers, who showed a locus of C_P minima for the $n - m$ Lennard-Jones (LJ) fluids in the supercritical part of the temperature-density phase diagram [50,54]. The reason why a C_P minimum has not previously been observed in either the LJ fluid or real fluids is possibly because the magnitude of the minimum is much less pronounced than that of the maximum.

Note that in LJ and LJ-like fluids there is also a minimum in C_V and maximum in C_V and C_P, whose presence may be a consequence therefore of the attractive part of the potential. An attractive part in the interparticle potential is necessary for the appearance of a maximum in C_V [50,54,55]. The appearance of a minimum in the density dependence of C_P for the soft-sphere fluids suggests a nontrivial origin which could extend to other types of purely repulsive particle fluid. It is noteworthy that C_P is one of the richest potential sources of information on the detailed processes taking place in molecular systems and also one of the hardest to understand in physical terms compared to other major thermodynamic quantities [56–58]. Furthermore, it is commonly measured in macromolecules such as proteins [59]. Therefore, the discovery of qualitatively new behavior in this thermodynamic property could have useful implications from fundamental and practical points of view.

III. MD SIMULATIONS

As shown in the previous section, to obtain the major thermodynamic properties of the soft-sphere system, it is sufficient to know the compressibility factor Z and its density derivative. In practice, because $Z = nu/3$, where $u = \langle U\rangle/Nk_BT$, the task reduces to the accurate determination of $u(n,\zeta)$ from which the derivative of Z can be obtained numerically. The most accurate values of u in the entire softness-density domain can be obtained from MD or Monte Carlo simulations. An extensive series of MD calculations has been performed for a large number of IP systems covering essentially the whole range of softness, $0 < s < 1/3$ or $\infty > n > 3$. Most of the calculations where performed up to the freezing density, ζ_f. The fluid-solid coexistence line for the soft-sphere fluid as a function of n was determined by Agrawal and Kofke [28] and the coexistence fluid and solid packing fraction, ζ_f and ζ_s were also obtained from that work.

In the range $0 < \zeta < \zeta_f$, depending on n, the simulations were performed for at least 16 and up to 33 equally spaced densities, and additional calculations were performed for some n values in the low density and dense fluid regions. The *NVE***PG** MD simulations were carried out on particles interacting using the soft-sphere potential of Eq. (1), with the potential exponent values going down to $n = 4$. The simulations were carried out mostly with $N = 4000$ particles, but for $n \leqslant 5$ the system consisted of $N = 6912$, which was necessary because of the relatively long range of these particular potentials. In this study the reduced temperature, $T^* = k_BT/\epsilon = 1$, and quantities are given in terms of the basic units of σ, ϵ, and m, the mass of a particle, i.e., energy in ϵ, time in $\sqrt{m\sigma^2/\epsilon}$, and the self-diffusion coefficient D in $\sqrt{\sigma^2\epsilon/m}$. The interaction truncation distance, r_c, was where the potential was 0.0001 (for $n = 4.5$ and 4 it was 0.001 and 0.002, respectively). The long range correction for energy was calculated from the tail of the radial distribution function $g(r)$ and for dilute systems $g(r > r_c) = 1$. The equations of motion were integrated with the leapfrog Verlet algorithm with a time step of $dt = 0.001$ for $n > 12$ and $dt = 0.005$ for $n < 12$. The averages were calculated from well-equilibrated simulations of length 4×10^5 time steps. The accuracy of the resultant Z is estimated to be better than $\leqslant 0.2\%$. For some (n,ζ) points calculations of Z were performed with a range of system sizes, $N = 824$, 1310, 2048, 4000, and 6912 particles. The difference between the value of the property for $N = 4000$ and 6912 was always within the estimated error bar from which it was concluded that $N = 4000$ is for practical reasons representative of the thermodynamic limit.

For an N-particle system,

$$u = \frac{1}{2Nk_BT}\left\langle \sum_{i=1}^{N}\sum_{i\neq j}^{N}\phi(r_{ij})\right\rangle, \tag{12}$$

where r_{ij} is the separation between particles i and j and $\langle\cdots\rangle$ denotes the simulation average. For convenience later, note that the compressibility factor is defined as in Table I *without* the usual kinetic component, i.e., $Z \equiv P/\rho k_BT - 1 = nu/3$. The

TABLE II. The coefficients obtained from the 8th-order polynomial fit to the simulation data. The hardness of the potential is n, C_i is the polynomial coefficient, and ζ_f is the fluid packing fraction at fluid-solid coexistence. For $n = 4,4.5$ the 12th-order polynomial was applied and the coefficients $[C_9, C_{10}, C_{11}, C_{12}]$ were $[-13.4741, 2.896\,95, -0.363\,64, 0.020\,22]$ and $[-17.4563, 4.496\,05, -0.679\,67, 0.045\,71]$, respectively. For $n \geq 5$ the coefficients C_1 and C_2 are fixed by the virial coefficients B_2 and B_3, respectively.

n	C_1	C_2	C_3	C_4	C_5	C_6	C_7	C_8	ζ_f
4.00	14.6574	28.2509	−48.1149	87.3579	−120.581	119.300	−83.3504	40.6152	2.976 70
4.50	10.7527	26.4590	−32.4275	57.3235	−85.2114	95.2146	−77.1051	44.2369	2.203 00
5.00	8.872 64	24.1805	−14.6300	16.7896	−15.3927	9.124 22	−3.031 88	0.42626	1.729 40
6.00	7.089 82	20.2513	9.604 30	−17.3478	23.1920	−19.9470	9.638 66	−1.972 35	1.218 40
6.70	6.439 49	18.5335	17.5447	−16.2752	16.0200	−11.5328	4.810 37	−0.822 88	1.027 70
8.00	5.738 08	16.5986	22.1669	7.223 71	−22.9436	36.6872	−33.2332	12.5396	0.825 10
12.00	4.901 67	13.8282	24.2072	31.0571	8.131 78	35.6480	−60.0180	34.9080	0.610 20
18.00	4.515 15	12.3269	23.9940	22.2987	97.6522	−92.9930	169.189	−38.8922	0.53140
36.00	4.222 19	11.0585	19.4627	63.7843	−201.561	987.482	−1622.70	1364.72	0.492 40
72.00	4.103 35	10.5017	20.8288	7.772 51	194.470	−347.378	426.670	267.538	0.487 00

self-diffusion coefficient was calculated from the long time limit of the mean square displacement of particle positions [1]. Additionally, for $n = 12$ and a few selected densities, the isothermal heat capacity, C_V, was calculated from the energy fluctuations in the canonical ensemble, *NVT*. The calculations of C_V were performed with system of $N = 4000$ particles. The equations of motion were integrated with the velocity Verlet algorithm with Nosé-Hoover thermostat [60] using a time step of $dt = 0.001$. The averages were calculated from well-equilibrated runs of length 2×10^6 time steps.

IV. RESULTS AND DISCUSSION

The compressibility factors calculated by MD, Z_{MD}, for a range of n values were fitted to a polynomial, $Z_{\mathrm{poly}}(\zeta) = \sum_i^M C_i \zeta^i$, where the polynomial coefficients are given in Table II ($M = 12$ for $n < 5$ and $M = 8$ for $n \geq 5$). For all the soft-sphere fluids considered, the polynomial function $Z_{\mathrm{poly}}(\zeta)$ was within the error bars of the MD points and $|Z_{\mathrm{poly}} - Z_{\mathrm{MD}}| < 0.001$.

The density derivative of Z was calculated numerically from the Z_{MD} data using the standard four-point method of differentiation and the resultant Z'_{num} is given along with Z_{MD} data in the Supplemental Material [61]. $Z'_{\mathrm{poly}} = \sum_{k=1}^{M-1} k C_k \zeta^{k-1}$ represents Z'_{num} in the density-softness plane with accuracy better than 0.05. Such accuracy is sufficient for purposes of this work, and thus in what follows Z, Z' are represented by Z_{poly} and Z'_{poly} (consequently, in calculations of the thermodynamic properties the coefficients in Table II are required only).

A. Thermodynamic properties

The known Z and Z' can be used to obtain all basic thermodynamic properties of soft-sphere fluids from the expressions given in Table I. Formally, any thermodynamic property, $\mathcal{A}$, of the soft-sphere system can be considered to be a surface, $\mathcal{A}(n, \zeta)$, which in the figures below is shown as the projection $\mathcal{A}$ vs ζ/ζ_f.

The results for B_T and B_S for the soft-sphere fluids are presented in Fig. 1. The ratio, $B_T/\rho k_B T$ is a monotonically increasing function of both ζ and the softness parameter, s. It is bounded from below by the result for the HS fluid and increases unboundedly for $n \to 3$, which can be attributed to the behavior of the second virial coefficient in this limit, as

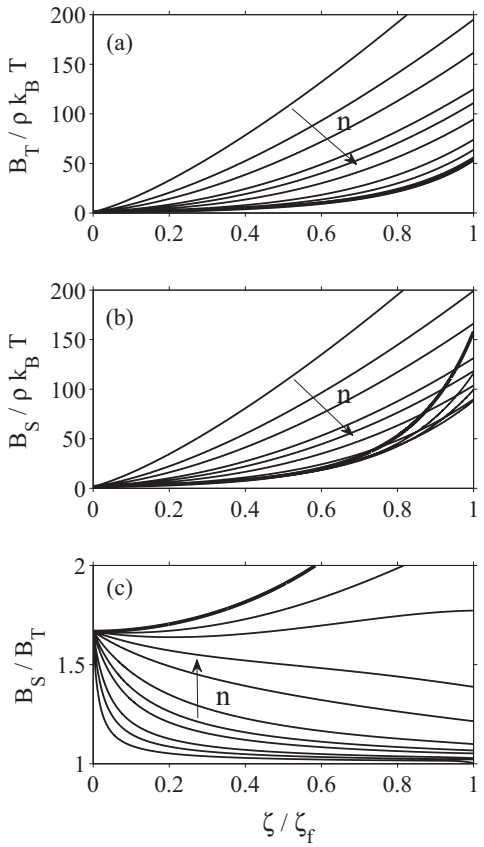

FIG. 1. Thermodynamic properties as a function of ζ/ζ_f: (a) isothermal bulk modulus B_T (the inverse isothermal compressibility), (b) adiabatic bulk modulus B_S (the inverse adiabatic compressibility), and (c) the ratio B_S/B_T. The solid lines show $B_T/\rho k_B T$, $B_S/\rho k_B T$, and B_S/B_T for several representative values of $n = 4$, 4.5, 5, 6, 6.7, 8, 12, 18, 36, 72, and ∞. In the figure the direction of increasing n is indicated by the arrow. The bold solid line is the HS limit. The maximum value of the ratio, B_S/B_T is at HS freezing and is approximately equal to 2.88.

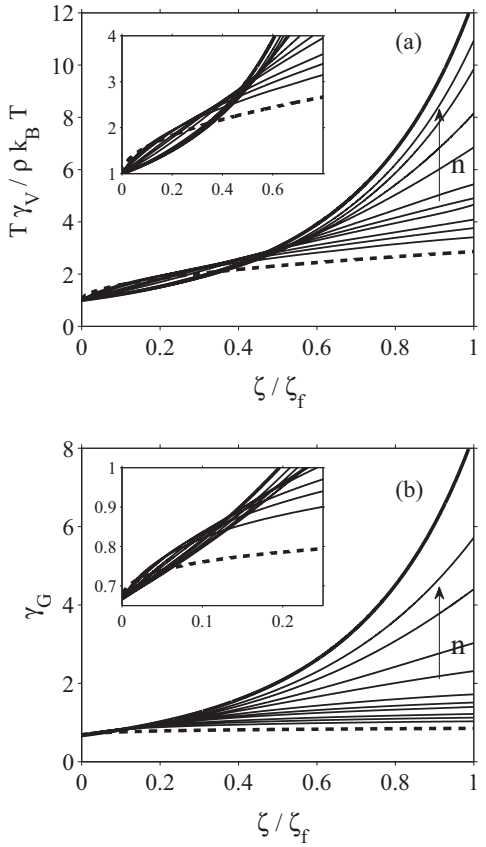

FIG. 2. Isothermal pressure coefficient γ_V and Grüneisen parameter γ_G, both as a function of ζ/ζ_f. The solid lines show $T\gamma_V/\rho k_B T$ (a) and γ_G (b) for the same n values as in Fig. 1. The bold solid line is the HS limit, and the dashed line represents the prediction for the $n \to 3$ limit. In the insets enlargements of the low and intermediate density regions are shown.

$B_2(n \to 3) \to \infty$. The behavior of the adiabatic bulk modulus, $B_S/\rho k_B T$, is similar apart from the nonmonotonic softness dependence close to the fluid-solid boundary.

The ratio B_S/B_T is shown in Fig. 1(c). This trend follows from the low density limit, $\frac{5}{3} - \frac{4}{3}(\frac{5}{n} - \frac{6}{n^2})B_2\zeta$, in that it has an initial nonpositive slope which increases in magnitude with softness. For most soft-sphere fluids B_S/B_T is a purely decreasing function of density across the whole fluid region. Only for steeply repulsive ($n \gg 1$) soft-sphere fluids does the ratio start to increase at higher densities. The ratio for the HS fluid is a monotonically increasing function of density which acts as an upper bound of this function for all n. Note that on increasing softness the ratio decreases markedly towards unity and the limiting case at low density is $\frac{B_S}{B_T}(n \to 3, \zeta > 0) = 1$. Thus, the characteristic feature of very soft-sphere fluids is $B_S \approx B_T$ for all densities apart from in the very dilute region.

The isothermal pressure coefficient and the Grüneisen parameter are shown in Fig. 2. Both quantities increase with density and are bounded by their low density limits and the HS values at freezing densities. The density dependence in both cases changes from a convex form for the steeply repulsive fluids to one which is concave and fairly flat for the small n-value fluids. At lower densities the hardness dependence of both properties is weak. By "convex" we use the standard

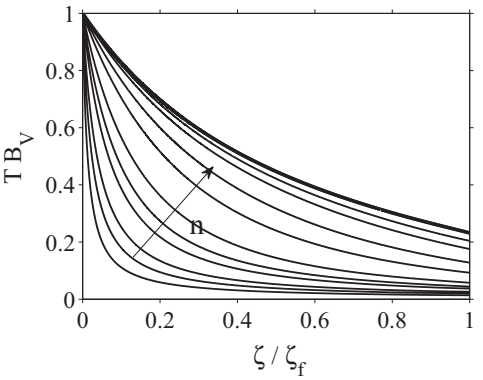

FIG. 3. The volume expansivity coefficient, B_V vs ζ/ζ_f. The solid lines show the TB_V for different $n = 4, 4.5, 5, 6, 6.7, 8, 12, 18, 36, 72$, and ∞. The bold solid line is the HS limit.

mathematical definition that the gradient of the function increases with density, while "concave" means the opposite trend.

As explained in Sec. II, the values of the volume expansivity, which is defined as the ratio $B_V = \gamma_V/B_T$, are limited to the interval $(0; 1/T)$, so, as may be seen in Fig. 3, the quantity $TB_V(n,\zeta)$ decreases monotonically from unity with density and softness, as expected. The HS fluid is the upper limit of this thermodynamic property. For very soft fluids the product decreases rapidly towards zero with the limit $TB_V(n \to 3, \zeta > 0) = 0$. This limit may be deduced from the fact that $B_T(n \to 3, \zeta) \to \infty$ and that the isothermal pressure coefficient hardly changes with density for $n \to 3$, as seen in Fig. 2(a).

The Joule-Thomson coefficient is shown in Fig. 4. As explained in Sec. II, it must always be negative for the soft-sphere system. As may be seen in the figure, for each n value, this thermodynamic property increases monotonically with density from its initial value of $k_B\mu_{JT}(n, \zeta = 0) = -4\pi(1 + 3/n)\Gamma(1 - 3/n)/15$ to one greater than ca. –0.25 at the freezing density. At low densities the rate of increase with density is considerable, particularly for very soft fluids

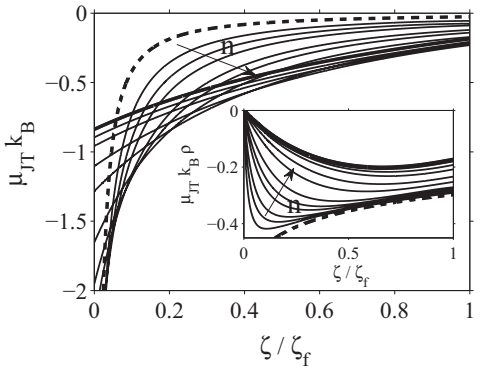

FIG. 4. The Joule-Thomson coefficient μ_{JT} vs ζ/ζ_f. The solid line is $\mu_{JT}k_B$ for the same n values as in Fig. 3. The bold solid line is the HS limit and the dashed line represents the prediction for the $n \to 3$ limit. The inset shows $\mu_{JT}k_B\rho$ vs ζ/ζ_f, where the data are taken from the main graph.

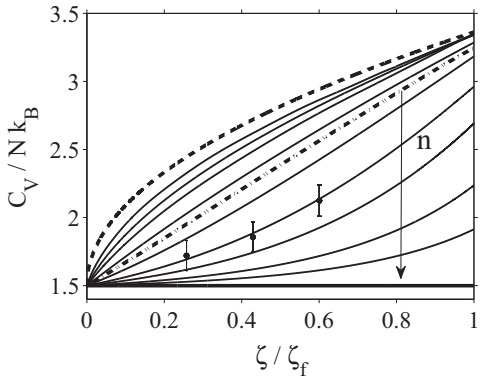

FIG. 5. Isochoric heat capacity C_V vs ζ/ζ_f. The solid lines show C_V/Nk_B for different $n = 4$, 4.5, 5, 6, 6.7, 8, 12, 18, 36, 72, and ∞. The bold solid line is the HS limit, the dot-dashed line represents the quasilinear trend for $n = 6.7$, and the dashed line is the predicted limit for $n \to 3$. The three solid circles with error bars are the *NVT* simulation data calculated from energy fluctuations for $n = 12$.

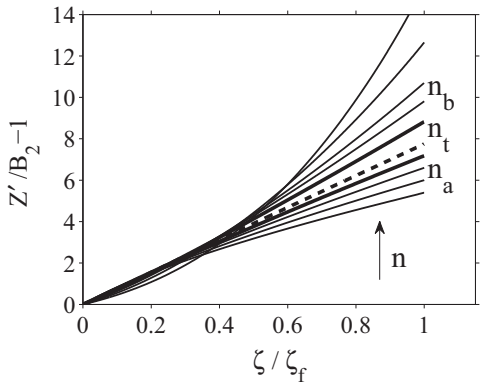

FIG. 6. The function $y = Z'/B_2 - 1$ vs ζ/ζ_f. The solid line is the function y for $n = 5.0$, 5.2, 5.4, 5.6, 5.8, 6.2, 6.6, 7, 8, and 10. The dashed line shows the quasilinear behavior of y for $n_t = 5.8$. The bold solid lines separate the convex, intermediate, and concave domains, where $n_a = 5.6$ and $n_b = 6.2$.

but at larger densities in the range $\zeta/\zeta_f \gtrsim 0.6$ the density dependence of μ_{JT} becomes weak for all n. In fact, the HS fluid (the bold solid line on the figure) has the weakest density dependence, and in this limit the Joule-Thomson coefficient can be approximated well by a simple almost flat function of the empirical form, $k_B\mu_{JT}(\frac{1}{n} = 0,\zeta) \approx -4\pi/15 + 120\zeta + 96\zeta^2$.

In the inset the product $\mu_{JT}k_B\rho$ is shown to indicate the role of density in the behavior of μ_{JT} in the low density region (see Table I).

The isochoric heat capacity $C_V(n,\zeta)$ shown in Fig. 5 is a monotonically increasing function of density as well as of softness. On increasing n the functional form goes from concave to convex, and the limiting form is the constant ideal gas value for the HS fluid. For very soft spheres it is observed that $C_V \sim \zeta^\alpha$ with $\alpha \to 0.5$, which is consistent with our previous studies on the EoS of soft fluids in this limit [62], where it was argued that the limiting form is $Z(n = 3,\zeta) = B_2\zeta + c\zeta^\alpha$ and $\alpha \approx 0.5, c \approx 1.5$. As $B_2(n \to 3) \to \infty$ both Z and Z' also tend to ∞. However, a combination of these two quantities, such as $Y = Z - 3\zeta Z'/n \to C\zeta^\alpha$, where $C = (1-\alpha)c$, is finite. This property enables the $n \to 3$ behavior of all of the above thermodynamic properties to be understood. In particular, the following have a finite limit even in the $n \to 3$ limit, $C_V/Nk_B \to 1.5 + C\zeta^\alpha$, $T\gamma_V/\rho k_B T \to 1 + C\zeta^\alpha$, $\gamma_G \to (1 + C\zeta^\alpha)/(1.5 + C\zeta^\alpha)$, and $TB_V \to 0$. In the case of the Joule-Thomson coefficient we first note that in the $n \to 3$ limit, $Z/B_2 \to \zeta$, $Z'/B_2 \to 1$, and $\text{const}/B_2 \to 0$ and therefore, $\mu_{JT}(n \to 3,\zeta) \to -\pi/3\zeta[3 + 2(Z - \zeta Z')] = -\pi/3\zeta[3 + 2C\zeta^\alpha]$. The predicted $n \to 3$ limit of the thermodynamic properties is marked in the figures as a solid bold dashed line.

The excess entropy of the soft-sphere fluid is defined through $S_{ex}/Nk_B = -\int_0^\zeta Z/\zeta' d\zeta' + Z$ which tends to $-2C\zeta^\alpha$ in the $n \to 3$ limit. The excess entropy per particle in units of k_B, hereafter denoted by S, is the total entropy minus the ideal gas contribution.

The convex or concave form of the heat capacity means that its second derivative is positive for the steeply repulsive and negative for very soft fluids or, alternatively, that the expression $(n-6)Z'' - 3\zeta Z''' = Y''$ is positive or negative for all fluid densities, respectively. Thus, there are three softness intervals which have qualitatively different behavior in the derivatives of the major thermodynamic properties (which involve Y). Recall that because for the IP system, $Z(\zeta \leqslant \zeta_f; n)$ is a convex (positive and monotonically increasing) function of density, its first and second derivatives are always positive. If for a given n, Z' is convex or concave, then the third derivative must be positive or negative, respectively. In Fig. 6 the function $y = Z'/B_2 - 1$ is plotted as a function of density, from which it is concluded that Z' is concave for $n < n_a \approx 5.6$ and convex for $n > n_b \approx 6.2$. Therefore, for $n < n_a$, the functions Z, Z', Z'' are positive and $Z''' < 0$, and for $n > n_b$ all these functions are positive. Thus, the thermodynamic properties of soft-sphere fluids are combinations of the convex Z and Z', which is convex or concave at all densities or displays mixed convexity in different density regions. As a result, qualitatively different behavior in the derivatives of the major thermodynamic properties can be observed usually for three different softness intervals defined through the n values, (n_a,n_b). In the case of the directly linked properties $Y, C_V, T\gamma_V/\rho k_B T$ these are (6.3,8), and in the case of S it is (6.2,6.7).

It is noteworthy that if for a given thermodynamic property, $\mathcal{A}(n,\zeta)$, the convex and concave regions exist, then a transition from one to the other form takes place in an intermediate n region often through a quasilinear ridge in (n,ζ) space. In other words, there exists a particular transitional (t) softness or n range, n_t, where there is $n_a < n_t < n_b$ for which $\mathcal{A}(n = n_t,\zeta) \sim \zeta$. The exact density dependence is not strictly linear (see Fig. 6), but the nonlinear part seems to be marginal at this particular softness value or nearby softness values. The observed near linearity in $C_V/Nk_B \sim \zeta$ for certain intermediate n values has several consequences. First of all, this is equivalent to $Y = K\zeta$ and to a form for the compressibility factor, $Z_{\text{lin}} = B_2\zeta + C\zeta^{n/3}$, where C is a constant, and which is the solution of the differential equation for C_V or Y, i.e., $-3\zeta Z'/n + Z - K\zeta = 0$, where $K = (1 - \frac{3}{n})B_2$. Next, it follows directly from the definition

of S that if $Y = K\zeta$ then also $S = K\zeta$, so that if quasilinear behavior is observed in C_V for n_t it will also be present in S for the same softness.

The value of n_t and the constant C can be estimated as the "coordinates" of the minimum on the surface $\mathcal{E}(n,C) = \int |Z_{\rm MD} - Z_{\rm lin}| d\zeta$, from which the most linear density behavior in C_V and S was found to be for $n_t \cong 6.4$ and $C = 26.11$. As the mixed convexity region is narrow it can be approximated by a single value of n_t. Thus, $\mathcal{A}(n_t,\zeta)$ can be considered to be an approximate demarcation line, above and below which the thermodynamic properties (for example, C_V and S) of soft-sphere fluids exhibit a qualitatively different density dependence, i.e., convex and concave, respectively.

It is notable that the linearity in $C_V(\zeta)$ for a given n means also that, $\langle U\rangle/Nk_B = \rho\frac{\pi}{2n}B_2T^{(1-3/n)} + (\rho\frac{\pi}{6})^{n/3}3C/n$, which comes from a straightforward reformulation of $Z_{\rm lin}$. In turn, from this temperature dependence $\langle U\rangle \sim T^{(1-3/n)}$, the expression $C_V \sim T^{-3/n}$ can be derived. Rosenfeld and Tarazona predicted from density functional theory that the energy on the isochore is of the form $U(\rho,T) = a(\rho) + b(\rho)T^{3/5}$ and consequently $C_V \sim T^{-2/5}$ [63]. Thus, the Rosenfeld and Tarazona result, $\langle U\rangle \sim T^{0.6}$, predicts linearity of C_V for $n = 7.5$, which is reasonably close to the value $n \approx 6.7$ for which a linear behavior in C_V is observed. The behavior of C_V in Fig. 5 indicates that the equation, $U = a + bT^{3/5}$ is obeyed well for almost the whole IP fluid range for intermediate values $6 < n < 8$. Also, it may represent reasonably well the IP fluid data for other n but only in limited ranges of ζ or (ρ,T) plane. Thus, from Fig. 5 it may be seen directly that, apart from intermediate n values and particularly for the steeply repulsive IP fluids, the relation $\langle U\rangle \sim T^{(1-3/n)}$ and consequently $C_V \sim T^{-3/n}$ can be fulfilled only locally or in a limited range of ζ and its performance should be better for dense fluids (close to freezing).

B. Minimum in heat capacity, C_P

The last thermodynamic property to be considered is the isobaric heat capacity, C_P. Some general features of C_P follow directly from the formula given in Table I, its low density expansion in Eq. (11) and from the thermodynamic relation $C_P = C_V B_S/B_T$. The isobaric heat capacity of the HS fluid is a monotonically increasing function of density from the minimum value of 2.5 at $\zeta_{\rm min} = 0$. It is the upper limit of the C_P for all n in the whole fluid phase.

For very soft spheres, the ratio B_S/B_T tends to unity which means that $C_P(n \to 3,\zeta) \to C_V(n \to 3,\zeta) \to 1.5 + C\zeta^{0.5}$. Thus, for very soft fluids $C_P \approx C_V$, apart from in the very dilute region where $C_P(\zeta \to 0)$ must tend to 2.5. The discussion in Sec. II on the low density expansion of the isobaric heat capacity indicates this property should have a minimum at lower densities.

Figure 7 shows $C_P(n,\zeta)$ calculated from the MD results for Z and Z'. All of the predicted features of this thermodynamic property mentioned above are clearly evident in the figure. The low density region is enlarged and the locus of the minima, i.e., the line $C_P(n,\zeta_{\rm min})$, is presented in different projections in Fig. 8 to make clear different aspects of this particular region. In all projections the minimum line is qualitatively similar to that predicted by the analytic expression in Eq. (11)

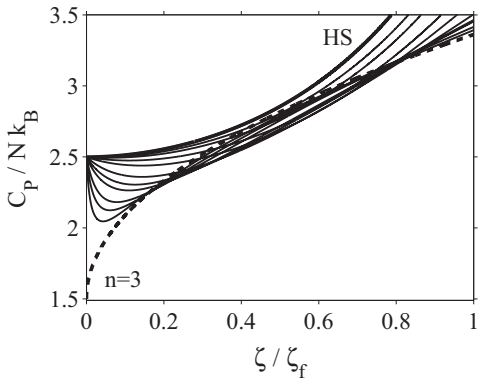

FIG. 7. Isobaric heat capacity $C_P(n,\zeta)$ vs ζ/ζ_f. The solid lines show the $C_P(n,\zeta)/Nk_B$ for $n = 4, 4.5, 5, 6, 6.7, 8, 12, 18, 36, 72$, and ∞. The bold solid line is the HS limit, and the dashed line represents the predicted limit for $n \to 3$.

where only the lowest level density representation of $Z = B_2\zeta$ is used. For the steeply repulsive and very soft-sphere fluids the minimum shifts towards very small densities, $\zeta_{\rm min} \to 0$, so for these limiting softness values, C_P is expected to be approximated well by Eq. (11), which is what is observed in Fig. 8. A considerable difference occurs for intermediate softness values particularly in the range $5 < n < 20$, where the minimum shifts towards higher densities, up to $\zeta/\zeta_f \approx 0.15$ for $n = 10$. The use of more terms in $Z = \sum_{i=1}^{M} B_{i+1}\zeta^i$, where $M = 2,3,4$, gradually improves the analytic representation of

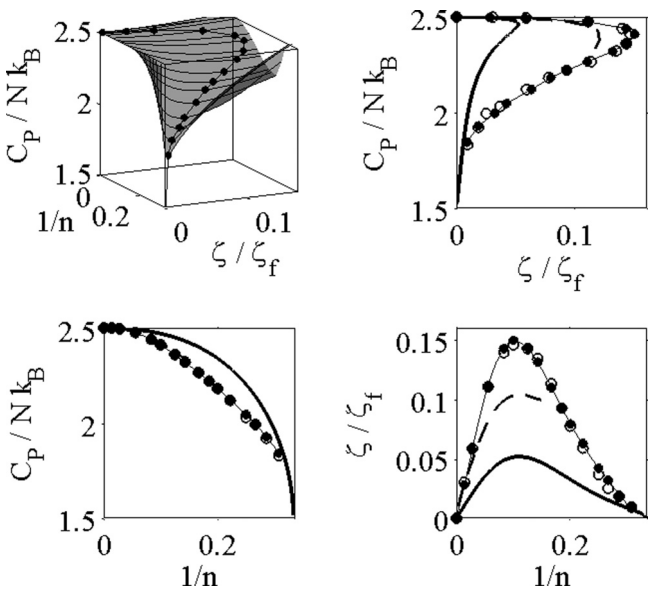

FIG. 8. The minimum line in the isobaric heat capacity, $C_P(n,\zeta)$, shown from different projections. The top left panel presents the surface of $C_P(n,\zeta)$ for small density. The top right panel shows the $C_P - \zeta/\zeta_f$ projection. The bottom left panel shows the $C_P - 1/n$ projection, and the bottom right panel is the $\zeta/\zeta_f - 1/n$ projection. The solid dots represent the position of the minimum (the thin line is a fit to these data). The bold solid and dashed lines are the minimum lines obtained for the virial approximation $Z = \sum_1^M B_{i+1}\zeta^i$ with $M = 1$, 3, respectively. The open circles are solutions for the $Z_{\rm MD}(\zeta \ll \zeta_f)$ represented by a third-order polynomial.

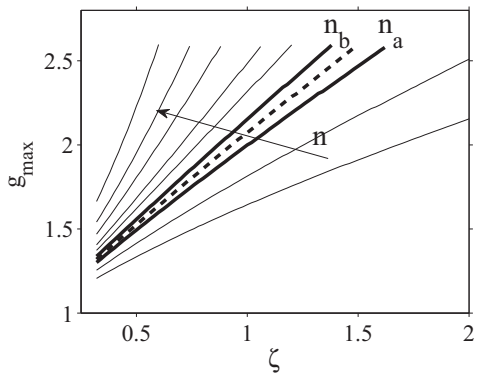

FIG. 9. The density dependence of the maximum of the first peak in radial distribution function $g(r)$ for different hardness values, $n =$ 4, 4.5, 5, 5.2, 5.4, 5.8, 6.2, 7, 8, and 10. The dashed line follows the quasilinear behavior when $n_t = 5.2$. The bold solid lines separate the three different areas of convex to intermediate to concave behavior, where $n_a = 5.0$ and $n_b = 5.4$.

the minimum line and relatively good agreement is achieved already even for $M = 2$. However, for the softness $1/n \geqslant 0.2$ no solution exists to represent C_P by the virial sum which can probably be attributed to a poor convergence of the virial series and perhaps a smaller radius of convergence for very soft-sphere fluids [31]. The known difficulty with resummation of the virial series for more soft interactions led to the proposal of alternative resummation methods [30,31] or the idea of "effective" virial coefficients [22]. Replacing B_3 and B_4 with effective coefficients b_2^e and b_3^e (obtained from fitting the low density $Z_{\rm MD}$ data), we find for $Z = B_2\zeta + b_2^e\zeta^2 + b_3^e\zeta^3$ that the minimum in C_P exists for all softness values in this case. These minima shown for selected softness in Fig. 8 as open circles are close to the minima line.

C. Structural properties

The existence of the demarcation line in the Z' surface appears to be one of the key factors which determines the softness dependence of the thermodynamic properties, and in some cases in a rather direct way. This influence may be expected as the thermodynamic properties depend explicitly on Z' as seen in Table I. Because of the relation $Z = \frac{4\zeta}{k_B T}\int \phi' g(r;n,\zeta) r^3 dr$, one might expect that the behavior of $Z'(n,\zeta)$ can to some extent be related to the softness dependence of the radial distribution function, $g(r;n,\zeta)$ and/or its density derivative, $\partial g/\partial\zeta$.

Figure 9 demonstrates that a basic structural property, the value of the first peak maximum in the radial distribution function, $g_{\rm max}$, behaves in a way similar to the thermodynamic properties. Three qualitatively different softness regions may be distinguished, where in this case $n_a = 5.0$ and $n_b = 5.4$. It had been established previously that at low densities the character of $g(r)$ changes from being oscillatory to monotonic in r with decreasing density [27]. This crossover packing fraction varies approximately as $\zeta_c \approx 0.5/n^{1.5}$. For $\zeta < \zeta_c$ there is no maximum in $g(r)$ for any n value, so in Fig. 9 only the smaller density range $\zeta > 0.25$ is considered. Note also that for this property the demarcation line between convex and concave behavior extends up to the fluid coexistence

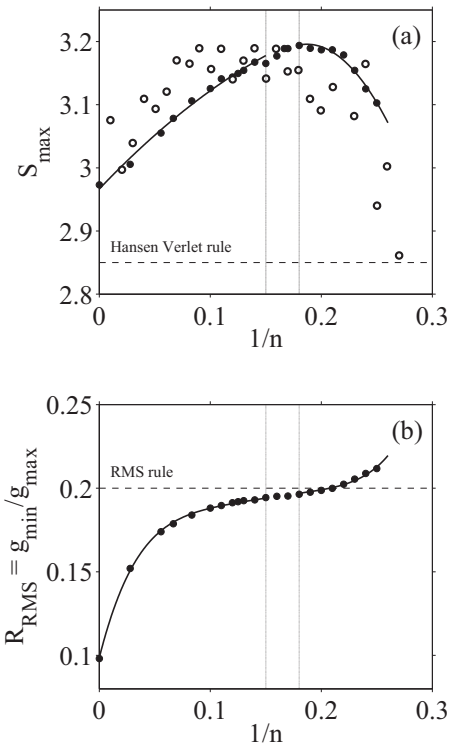

FIG. 10. Test of (a) the HV freezing rule condition, $S_{\rm max}$ vs $1/n$, and (b) the RMS freezing rule criterion, $g_{\rm min}/g_{\rm max}$, as functions of $1/n$. The solid circles are the MD data and the open circles are the result of Agrawal and Kofke [28]. The vertical thin lines indicate the intermediate softness region, $5.6 < n < 6.2$.

packing fraction value, ζ_f. Consequently, this effect should be present in some freezing criteria, particulary those which are formulated in terms of $g_{\rm max}$ or related to $g(r)$ in some other way.

Two well-known freezing criteria, the Hansen-Verlet (HV) freezing rule [64] and that of Raveché-Mountain-Street (RMS) [65], are tested in Fig. 10 for the range of n values. The HV rule states that the first maximum of the structure factor $S_{\rm max} \approx 2.85$ at freezing, while according to RMS, the ratio of the first minimum to the first maximum of the radial distribution function, $R_{\rm RMS}$, at freezing is $\approx$0.2. Figure 10 demonstrates that in the case of the IP fluid both $S_{\rm max}$ and $R_{\rm RMS}$ depend markedly on the softness. This dependence correlates well with the softness dependence observed in $g_{\rm max}$; in particular, three softness zones can be seen and the narrow intermediate region is located within the range, $5.6 < n < 6.2$.

In calculations of $S_{\rm max}$, the tail of $g(r)$ was first incorporated by assuming the contribution from the smallest pole solution representing the long distance decay is dominant in that r region [66]. The decay or tail of the radial distribution function $g(r)$ then has the form $A\exp(-\alpha r)\cos(\omega r + \delta)/r$, and the one-pole representation is a good approximation of $g(r \gg 1)$ at high densities, particularly close to the freezing density. The nonlinear procedure of curve fitting was used to perform fitting of the MD $g(r)$ data to determine A, α, ω, and δ. The structure factor, $S(q)$, is the Fourier transform of the radial distribution function $g(r)$ which was calculated in two parts, numerically for $0 < r < R$ and from the analytic

form of the tail for $R < r < \infty$. The distance, R, was chosen where the form $A\exp(-\alpha r)\cos(\omega r + \delta)/r$ is a good representation of $g(r)$ for larger radii. This approach allowed us to calculate accurately the softness dependence of $S_{\max}$ at freezing, shown in Fig. 10(a), which demonstrates the existence of the demarcation region in this quantity as well. A similar softness trend in $S_{\max}$ was noticed previously by Agrawal and Kofke [28], whose data are marked by open circles on Fig. 10(a). The HV rule seems to be a useful criterion for steeply repulsive and very soft interactions but cannot be considered to be a general freezing criterion. In the case of the RMS criterion, as may be seen in Fig. 10(b), the softness dependence of R_{RMS} is also well defined and changes from a concave to a convex form in the region around $n \approx 6.4$. Thus, this phenomenological criterion is not obeyed very well in soft-sphere systems either, particularly for steeply repulsive and very soft fluids, although to some extent it could be useful for the range $4 < n < 10$. The observed softness dependence of the major thermodynamic and also structural properties implies that the freezing criterion cannot be formulated simply in terms of these or directly related properties.

Finally, it is noteworthy that the range of intermediate softness in the freezing criteria established here corresponds well with the reported threshold of $n \approx 6$ below which the IP fluid freezes into a bcc solid and above which the fcc solid is the thermodynamically stable solid structure [17,28]. It is therefore possible that this threshold could be related to the convex-concave behavior of the density dependence of some thermodynamic properties but extensive calculations on IP solids would be needed to confirm this.

V. DIFFUSIVITY AND EXCESS ENTROPY

In this section the softness dependence of the self-diffusion coefficient is considered. The self-diffusion coefficient is problematic to measure experimentally, which has prompted interest in establishing possible relationships between it and thermodynamic quantities, $\mathcal{A}$, which are usually more readily measured. In fact, if such relationships could be established, we would already have an essentially analytic route (via Table I) to the self-diffusion coefficient directly from the EoS, i.e., $D(\mathcal{A}(Z,Z'))$. The choice S is motivated by a long-standing interest in establishing and exploiting a simple entropy scaling law for D, which is founded on the paradigm that a suitably scaled diffusion coefficient is a universal function of the excess entropy. More than 30 y ago, Rosenfeld [67] proposed a simple relationship between a normalized self-diffusion coefficient and the excess entropy per particle, S, which was based on analysis of data for model systems. The simple form is $D \approx a\exp(bS)$, where $a \approx 0.6$ and $b \approx 0.8$. This relationship, which is usually expressed in the form of $\ln(D)$ and S, is supported by many studies on various model and real fluids, including liquid metals and alloys [68]) but usually with different values for the constants, a and b [69–71]. This treatment has been applied to binary fluid mixtures [69,72,73], used to account for the region of diffusivity anomalies in waterlike model fluids [74–76] and to modify the Stokes-Einstein relation for liquid metals [77]. Therefore, this relationship appears to be widely applicable, even for inhomogeneous fluids and where there is particle confinement in channels of molecular dimensions [78,79]. Despite its phenomenological origin, this relationship has been widely used to provide an approximate estimate of D and is firmly established in the literature (see, e.g., Refs. [71,80]).

However, this formula has two main weaknesses. First, at low densities it differs from Enskog theory, which is known to account well for D in this domain, and predicts at low densities, $D \sim \zeta^{-1}$, for the HS fluid. For the soft-sphere fluid, a closed-form solution of the kinetic theory equations also exists for the $\zeta \to 0$ limit, and the first-order solution is $D = A_{01}/\zeta$, where

$$A_{01} = \frac{\sqrt{\pi}}{16}\left(\frac{2}{n}\right)^{2/n}\frac{1}{A_1(n)\Gamma(3-2/n)}, \tag{13}$$

and A_1 is a slowly varying function of n [70,81].

The next order approximation yields the coefficient, $A_{02} = A_{01}/(1-\varepsilon)$, to replace A_{01} above, where ε is a small correction term [81].

Second, in the dense fluid region (typically where, $S < -3$), $\ln(D)$ ceases to be linear in S. The magnitude of the deviation is less than in the $S > -1$ domain and, at least partially, could be explained by the limited accuracy of the experimental and simulation data. Nevertheless, this second deficiency is significant as it indicates that a simple exponential dependence between D and S fails for dense fluids, a point that was also raised as a possibility by Rosenfeld [70]. Thus, the relationship appears to be valid only in a limited range of excess entropies [82–84]. The first problem, the necessity to include the divergence in D at low densities, has led to the proposal of improved formulas [85–90]. Rosenfeld [70] argued that at very low densities the diffusion coefficient should be represented well (in these reduced units) by the inverse of S. It should be noted, however, that none of the existing empirical scaling relations for D in the literature correctly describes diffusion over the entire fluid range.

A simple and accurate representation of D in terms of S for the entire softness-density plane of soft-sphere fluids is proposed and tested here. Taking into account the various existing entropy scalings and the closed-form solution of the kinetic theory, a general representation is proposed,

$$D = \frac{A_0}{S}\exp(\Psi), \tag{14}$$

where Ψ is an unknown function of S with a property $\Psi(S \to 0) = 0$, and A_0 is chosen so that in the infinite dilution limit the kinetic theory prediction is recovered. The constant, $A_0 = 4A_{02}\Gamma(1-3/n)(1-3/n)$ is required to achieve the low density limit for D of the soft-sphere fluid. Analysis of the MD data for D revealed that for any softness the function Ψ in Eq. (14) is only weakly dependent on S and has a point of inflection which means that it cannot be accurately represented by a quadratic function. It was verified that it can be well-represented by a low-order polynomial of the form, $\Sigma_{i=1}^{M}\alpha_i S^i$. Importantly, our detailed analysis of $\ln(DS/A_0)$ against S has shown that an accurate representation of Ψ requires a fourth-order polynomial. A third-order polynomial representation of $\Psi(S)$ was insufficient for most of soft fluids, particularly in the range of $-S > 1$. Also adding additional terms ($M > 4$) does not significantly improve the accuracy of the polynomial representation of this function. The way

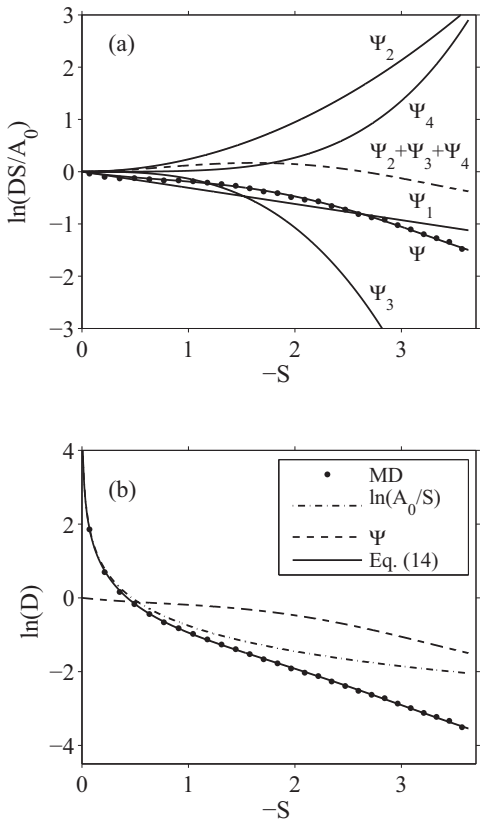

FIG. 11. Analysis of the diffusion coefficient, D, for $n = 6$ as a function of excess entropy using Eq. (14). (a) The polynomial $\Psi = \Sigma_{i=1}^{4}\alpha_i S^i$ with separate contributions, $\Psi_i = \alpha_i S^i$; (b) the separate contributions of the low density part A_0/S and $\exp(\Psi)$. The functions are shown on a ln-lin scale, the dots are the values obtained from MD simulation and the solid line is obtained from Eq. (14).

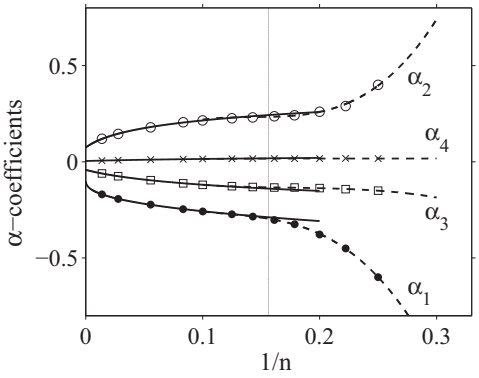

FIG. 12. The diffusion coefficient function, Ψ, expansion coefficients vs $1/n$. The symbols are the coefficients calculated with MD data. The vertical thin line indicates the value $n = 6.4$ near which the softness dependence of the parameters changes. The solid and dashed lines are the functions given in Table III.

in which these four terms contribute to Ψ as a function of S is demonstrated in Fig. 11(a) for $n = 6$. Defining $\Psi_1 = \alpha_1 S$, $\Psi_2 = \alpha_2 S^2$, $\Psi_3 = \alpha_3 S^3$, and $\Psi_4 = \alpha_4 S^4$, it is clear that the linear term is quite a good representation of Ψ only because the higher order terms mutually cancel to a large extent. However, the contribution, $\Psi_2 + \Psi_3 + \Psi_4$ is not negligible [see the dashed line in the Fig. 11(a)] and has to be taken into account to represent accurately D over the entire fluid range.

As shown in Fig. 11(b) the simulation values of $\ln(D)$ fall into two well-defined regions, which at low density can be represented by the $\ln(A_0/S)$ term and, at higher density, by the sum of $\ln(A_0/S)$ and the term produced by Ψ. At low densities, the Ψ term goes rapidly to zero and the dominant term is the two-body $\ln(A_0/S)$ contribution. In the domain $S < -1$, the contribution from the Ψ part becomes increasingly more important with increasing $-S$, which may be associated in part with nontrivial many-body contributions. The curvature of both contributions is similar but in the opposite sense, a feature which produces the approximate widely observed "universal" linear relationship. In fact, this is why the linear relationship seen between $\ln(D)$ and S is always only approximate, as it results from the overlap of two distinct regimes. The present analysis can therefore be used to interpret both positive and negative deviations from the universal linear behavior.

The behavior of $D(S)$ shown in Fig. 11 is very similar for all n values and quite similar to the D vs S correlations reported in the literature for other types of fluids. This suggests that the proposed model for $D(S)$ in Eq. (14) with $\Psi \cong \alpha_1 S + \alpha_2 S^2 + \alpha_3 S^3 + \alpha_4 S^4$ can be considered to be a minimal model which is able to account for all of the main features of the relationship between diffusivity and excess entropy.

Thus, in the case of the soft-sphere fluids the relationship between D and S can be made with four parameters (it requires at least four parameters). It was found that these parameters display a quite regular softness or $1/n$ dependence. Figure 12 shows that there are at least two features of note in the form of $\alpha_i(1/n)$. First, at any softness the magnitude of the parameter quickly decreases with the index which indicates the rapid convergence of the power series representation of the Ψ function. Second, near $n = 6.4$ the character of the softness dependence of all four parameters changes, which coincides with the value of n where the demarcation line in S occurs. Therefore, as for thermodynamic and structural properties there are three softness regions. For $n > 6.4$, the softness dependence is found to be represented well by $\alpha_i = a_i(1/n + d_i)^{k_i} + b_i$ and for $n < 6.4$ the optimal formula is $\alpha_i = c0_i + c1_i/n + c2_i/n^2 + c3_i/n^3$. In the narrow transition region around $n = 6.4$, the parameter values remain almost unchanged. Despite being the most obvious one to use, the fitting function adopted for Ψ is probably not unique and other expressions may match the data just as well. Having the explicit softness dependence of all α parameters a closed-form formula for the diffusion coefficient in terms of S, or $D(S(n,\zeta))$, for soft-sphere fluids has therefore been obtained. The accuracy of the proposed relationship [given in Eq. (14)], along with the coefficient values given in Table III, is demonstrated in Fig. 13 (the agreement between analytical and MD values for D is within 4%). Figure 13 also includes the recently proposed entropy-based relation [82], $D_{VMFS} = (a + bx)(1 + cx + dx^2)^{-1}\rho^{-1/3}$, where $x = \sqrt{-S}$, $a = 3.7521$, $b = -8.6910$, $c = 4.5594$, and $d = -1.6138$. This function can be seen to reproduce quite well the main

TABLE III. The coefficients obtained for the fit function, $\Psi = \Sigma_{i=1}^{4}\alpha_i S^i$ to the self-diffusion coefficient simulation data, $\ln(DS/A_0)$. For $n > 6.4$ the function is described by $\alpha_i = a_i(1/n + d_i)^{k_i} + b_i$, and for $n < 6.4$ by the polynomial $\alpha_i = c0_i + c1_i/n + c2_i/n^2 + c3_i/n^3$, $i = 1,2,3,4$.

	a_i	b_i	d_i	k_i	$c0_i$	$c1_i$	$c2_i$	$c3_i$
$i = 1$	−0.420 552	−0.098 498	0.000 000	0.418 637	−130.4095	49.841 11	−7.068 668	0.089 837
$i = 2$	−0.037 329	0.334 514	0.038 199	−0.595 241	56.933 95	−13.542 48	0.126 277	0.327 359
$i = 3$	1.370 355	1.151 654	0.022 647	0.036 688	14.095 61	−13.674 36	3.281 523	−0.364 936
$i = 4$	−9.591 840	0.019 655	1.471 870	−16.57 378	−6.215 103	4.1743 27	−0.865 069	0.073 335

features of $D(S)$ for soft fluids but for practically all of the softness values the predicted trend deviates noticeably from the actual $D(S)$ behavior obtained from the simulations.

An alternative description of the soft-sphere self-diffusion coefficient using the Adam-Gibbs (AG) formula was proposed by De Michele *et al.* [91], who computed the self-diffusion coefficient of atoms in a binary IP mixture which frustrates crystallization. They concluded from their calculations that in an intermediate softness regime the temperature dependence of the diffusion coefficient and configurational entropy can be scaled very well onto a single master curve with the adoption of an n-dependent reference temperature T_n and therefore with constant fragility. Analysis of our data indicates that, in general, T_n must be density dependent and that density and softness do influence the temperature dependence of the self-diffusion coefficient of the soft spheres and consequently also their fragility. However, there are regions of T (or density) where this dependence is weak and hardly detectable and such a scaling law may work reasonably well (such as the scaling law by Rosenfeld which approximates well the self-diffusion coefficient data for a range of density). Furthermore, to be more definite on the conclusions in Ref. [91], data in the supercooled region would be required but this region is not considered in our work.

VI. CONCLUSIONS

The work demonstrates that by applying the LTT [46,47] all the important thermodynamic properties of the soft-sphere system can be expressed in terms of the potential energy and its density derivative only (or equivalently Z and Z'). This provides new perspectives on the unique features of soft-sphere thermodynamics and enables relationships to be derived between the usual thermodynamic quantities which are not attainable via the conventional thermodynamic formula routes without this extra information.

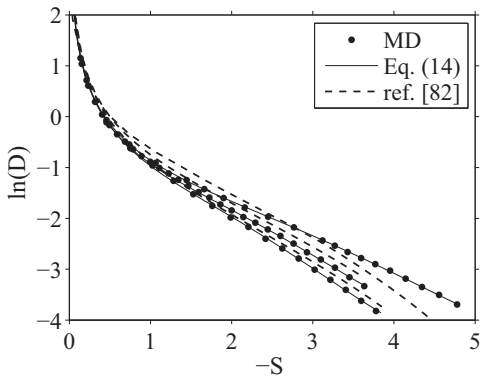

FIG. 13. Diffusion coefficient of the soft-sphere fluid as a function of the excess entropy. The dots are from the MD simulations and the solid line is the expression proposed in Eq. (14). The dashed line is the relation proposed by Vaz *et al.* [82]. The results are for $n = 5,12$ and ∞, from bottom to top, respectively.

From the relationships listed in Table I some general conclusions can be made. The Joule-Thomson coefficient of the soft-sphere fluid is always nonpositive and the volume expansivity cannot be greater than $1/T$. Also, the role of softness in the hard- and most soft-sphere ($n \to 3$) limiting cases is revealed clearly. Furthermore, the virial series representation of the compressibility factor, Z, can be used to express soft-sphere thermodynamics at low density fluids in analytical form.

In practice, the calculation of Z, Z' reduces simply to the accurate evaluation of the potential energy per particle $u(\zeta)$ which can now be achieved accurately and routinely by molecular simulation. Thus, the proposed approach considerably reduces the complexity involved in determining thermodynamic properties of this class of fluid and offers a practical means to explore soft-sphere thermodynamics across the whole softness-density domain. -

The isochoric and isobaric heat capacity, thermal expansion coefficient, isothermal and adiabatic bulk moduli, Grüneisen parameter, isothermal pressure, and Joule-Thomson coefficient of the soft-sphere fluid across the potential softness range are examined for new trends. These properties are monotonically increasing or decreasing functions of density. The exception is the isobaric heat capacity which displays a minimum at low densities. The existence of the minimum in C_P was reported only recently for the LJ-like model systems, and this is the first time it has been shown to be present for a purely repulsive potential.

For the stiffness parameter within the narrow range $5 < n < 8$ a quasilinear dependence on density is found for several thermodynamic properties. The quantity Z' displays a "transition" from a convex to concave form as the interaction potential becomes softer, which underpins a number of these trends. This qualitative difference in the softness dependence extends practically to the freezing density and was found to be present also in the height of the main peak, $g_{\max}$, of the radial pair distribution function (a key microstructural indicator). This has the consequence that freezing criteria based on the radial distribution function derived quantities are not expected to be universal. In fact, the soft-sphere fluid provides a simple and demanding test for the formulation of phenomenological freezing criteria.

A new and accurate formula has been proposed linking the self-diffusion coefficient to the excess entropy for the entire fluid softness-density domain. The widely observed "universal" linear relationship between $\ln(D)$ and S is shown always to be only approximate. Such a relationship has to take into account both the considerable increase of diffusivity at low densities and a non-negligible departure from linearity in the dense fluid region. To achieve these requirements the new expression incorporates the kinetic theory solution for the low density limit and an entropy-dependent function in exponential form to take account of finite density effects. It was found that this function depends only weakly on S and can be well-represented by a low-order polynomial whose coefficients display a similar softness dependence to Z'; i.e., three softness regions can be distinguished and the intermediate narrow region is in the vicinity of $n = 6.4$.

The results for thermodynamic properties, structural quantities, and diffusion coefficient indicate that three regions can be expected in the softness dependence of the physical properties (or their derivatives) of soft-sphere fluids with a narrow transition region within the range $5 < n < 8$.

It has been shown here for the soft-sphere fluid that the slope of the density dependence of certain properties increases with density for the stiffer potentials (convexity) and decreases with density for the softer range of potentials (concavity), with an almost zero change of slope domain in between. This observation and characterization could be useful in helping to interpret the behavior of the physical properties of various real and model liquids with density and pressure in diverse experimental fields, especially those where the soft-sphere scaling has already been applied to some extent. For example in tribology, the logarithm of the viscosity with pressure is well known to exhibit convexity, concavity, and mixed behavior for model lubricating oils at different temperatures [92–94] (a constant slope is equivalent to the Barus equation). Also, there are potential applications in geophysics and planetary science where the mineral equations of state are dominated by the repulsive part of the pair potential [95,96].

ACKNOWLEDGMENTS

The work has been supported partially by Polish National Science Center Grant No. DEC-2012/05/B/ST3/03255. Some of the simulations were performed at the Poznan Supercomputing and Networking Center (PCSS).

APPENDIX: DETAILS OF THE LTT METHOD APPLIED TO THE SOFT SPHERES

For the IP fluid, $\phi(r) = 1/r^n$, there is a unique relation between the configurational part of the compressibility factor, $Z = Z_{ex} = P/k_BT\rho - J$, and the potential energy, $U = \Sigma_i^{N-1}\Sigma_{j=i+1}^{N}\phi(r_{ij})$, through

$$Z = n\langle U\rangle/3Nk_BT = nu/3. \tag{A1}$$

For this potential all of the volume derivatives can be expressed in terms of the energy only. For any pairwise additive potential, the mth volume derivative has the form [46]

$$V^m\frac{d^mU}{dV^m} = \frac{1}{3^m}\Sigma_i^{N-1}\Sigma_{j=i+1}^{N}\Sigma_{k=1}^{m}a_{mk}r_{ij}^k\frac{d^k\phi}{dr_{ij}^k}, \tag{A2}$$

where the coefficients a_{mk} of the kth term of the mth volume derivative of the potential energy can be defined by the recursion relation as shown in the Meier and Kabelac work [46] and their first values are $a_{11} = 1$, $a_{21} = -2$, $a_{22} = 1$, $a_{31} = 10$, $a_{32} = -6$, and $a_{33} = 1$.

In the case of the IP potential, the derivatives are proportional to the potential,

$$\frac{d^k\phi}{dr^k} = \frac{(-1)^k n(n+1)\cdots(n+k-1)}{r^k}\phi = \frac{A_{kn}}{r^k}\phi, \tag{A3}$$

which gives

$$\begin{aligned} V^m\frac{d^mU}{dV^m} &= \frac{1}{3^m}\Sigma_i^{N-1}\Sigma_{j=i+1}^{N}\Sigma_{k=1}^{m}[a_{mk}A_{kn}\phi(r_{ij})] \\ &= U\frac{1}{3^m}\Sigma_{k=1}^{m}a_{mk}A_{kn}. \end{aligned} \tag{A4}$$

The first two derivatives are

$$V\frac{dU}{dV} = U\frac{1}{3}[a_{11}A_{1n}] = UC_{1n} = U\left(\frac{-n}{3}\right), \tag{A5}$$

$$\begin{aligned} V^2\frac{d^2U}{dV^2} &= U\frac{1}{3^2}[a_{21}A_{1n} + a_{22}A_{2n}] \\ &= UC_{2n} = U[2n + n(n+1)]/9. \end{aligned} \tag{A6}$$

These relations can be used to simplify the expressions for the Ω functions. The equality $E = \langle E\rangle = \langle K + U\rangle = \langle K\rangle + \langle U\rangle$ is used to write in a more basic form the averages $\langle U/K\rangle$ and $\langle U^2/K\rangle$,

$$\Omega_{00} = k_BT = \frac{2\langle K\rangle}{3N-3}, \quad \frac{\langle K\rangle}{Nk_BT} = \frac{3}{2}\left(1 - \frac{1}{N}\right), \tag{A7}$$

$$\Omega_{01} = \frac{N-1}{V}k_BT - \frac{C_{1n}}{V}\langle U\rangle = \frac{N-1}{V}k_BT + \frac{n}{3V}\langle U\rangle, \tag{A8}$$

$$\Omega_{20} = \left[\frac{3N-3}{2} - 1\right]\langle K^{-1}\rangle, \tag{A9}$$

$$\Omega_{11} = \frac{N-1}{V} + \left[1 - \frac{3N-3}{2}\right]\langle K^{-1}C_{1n}U\rangle/V \tag{A10}$$

$$= \frac{N-1}{V} - \left[1 - \frac{3N-3}{2}\right]\frac{n}{3V}\left\langle\frac{E-K}{K}\right\rangle \tag{A11}$$

$$\begin{aligned} = \frac{N-1}{V} - \left[1 - \frac{3N-3}{2}\right]\frac{n}{3V}[&\langle K\rangle\langle K^{-1}\rangle \\ &+ \langle U\rangle\langle K^{-1}\rangle - 1] \end{aligned} \tag{A12}$$

$$= \frac{N-1}{V} + \left[1 - \frac{3N-3}{2}\right]\frac{n}{3V} + \Omega_{20}\frac{n}{3V}(\langle K\rangle + \langle U\rangle) \tag{A13}$$

$$= \rho\left[\frac{N-1}{N} - \frac{n}{3}\left[\frac{3N-5}{2N}\right] + k_BT\Omega_{20}\frac{n}{3}\frac{(\langle K\rangle + \langle U\rangle)}{Nk_BT}\right], \tag{A14}$$

$$\Omega_{02} = \frac{2}{3V}\frac{N-2}{V}\langle K\rangle - \left[1-\frac{3N-3}{2}\right]\left\langle K^{-1}U^2C_{1n}^2\right\rangle/V^2$$
$$-\langle UC_{2n}\rangle/V^2 - 2\frac{N-1}{V}\langle UC_{1n}\rangle/V \quad \text{(A15)}$$
$$= \frac{2}{3V}\frac{N-2}{V}\langle K\rangle - \left[1-\frac{3N-3}{2}\right]$$
$$\times \frac{C_{1n}^2}{V^2}\left\langle\frac{E^2-2KE+K^2}{K}\right\rangle$$
$$-\frac{C_{2n}}{V^2}\langle U\rangle - 2\frac{N-1}{V^2}C_{1n}\langle U\rangle \quad \text{(A16)}$$
$$= \frac{2}{3V}\frac{N-2}{V}\langle K\rangle - \left[1-\frac{3N-3}{2}\right]$$
$$\times \frac{C_{1n}^2}{V^2}[E^2\langle K^{-1}\rangle - 2\langle U\rangle - \langle K\rangle]$$
$$-\frac{C_{2n}}{V^2}\langle U\rangle - 2\frac{N-1}{V^2}C_{1n}\langle U\rangle \quad \text{(A17)}$$
$$= \frac{2}{3V}\frac{N-2}{V}\langle K\rangle + \Omega_{20}\frac{C_{1n}^2}{V^2}(\langle K\rangle+\langle U\rangle)^2$$
$$+\left[1-\frac{3N-3}{2}\right]\frac{C_{1n}^2}{V^2}[\langle K\rangle + 2\langle U\rangle]$$
$$-\left[\frac{C_{2n}}{V^2}+2\frac{N-1}{V^2}C_{1n}\right]\langle U\rangle \quad \text{(A18)}$$
$$= \rho^2k_BT\left[\frac{2}{3}\frac{(N-2)}{N}\frac{\langle K\rangle}{Nk_BT} - \frac{n^2}{9}\left(\frac{3N-5}{2N}\right)\right.$$
$$\times\left(\frac{\langle K\rangle+2\langle U\rangle}{Nk_BT}\right) - \left.\left[\frac{C_{2n}}{N} - \frac{2(N-1)}{3N}n\right]\frac{\langle U\rangle}{Nk_BT}\right]$$
$$+\rho^2k_BTk_BT\Omega_{20}\frac{n^2}{9}\left(\frac{\langle K\rangle+\langle U\rangle}{Nk_BT}\right)^2. \quad \text{(A19)}$$

Thus, to calculate the Ω functions of the IP system only the two averages, $\langle U\rangle$ and $\langle K^{-1}\rangle$, are needed (as $\langle K\rangle$ can be replaced by T apart from a constant). Furthermore, $\Omega_{11} = C + D\Omega_{20}$ and $\Omega_{02} = A + B\Omega_{20}$, where $C = \rho(N-1)/N - \rho(3N-5)n/6N$, $D = \rho(\langle U\rangle + \langle K\rangle)n/3N = \rho k_BT[Z + n(N-1)/2N]$, $B = D^2$, and $A/\rho^2k_BT = \frac{(N-2)}{N}\frac{(N-1)}{N} - \frac{n^2}{12}\frac{(3N-5)}{N}\frac{(N-1)}{N} + \frac{\langle U\rangle}{Nk_BT}[\frac{n^2}{9}\frac{(3N-5)}{N} - C_{2n}/N + \frac{n}{3}\frac{2(N-1)}{N}]$. Next, $\langle K^{-1}\rangle$ is replaced with $d\langle U\rangle/d\zeta$, which can be achieved by noting that the IP thermodynamic properties depend on $\zeta = \frac{\pi}{6}\sigma^3\rho T^{-3/n}$ because of the unique scaling property of the soft-sphere system. Consequently, there is a relationship between the V and T derivatives,

$$-V\left(\frac{\partial P}{\partial V}\right)_T = \zeta\left(\frac{\partial P}{\partial \zeta}\right)_T = \rho k_BT\left[\zeta\frac{\partial Z}{\partial\zeta} + Z + J\right], \quad \text{(A20)}$$

$$T\left(\frac{\partial P}{\partial T}\right)_V = k_BT\left[(Z+J)\rho - \frac{3}{n}\rho\zeta\frac{\partial Z}{\partial\zeta}\right], \quad \text{(A21)}$$

which has the form

$$\frac{-V\left(\frac{\partial P}{\partial V}\right)_T - P}{T\left(\frac{\partial P}{\partial T}\right)_V - P} = -\frac{n}{3} \quad \text{(A22)}$$

or

$$B_T - P = \frac{n}{3}(P - T\gamma_V). \quad \text{(A23)}$$

This relation was exploited in Ref. [38] [Eq. (B10)], where $W = nU/3$ and, thus, $\partial\langle W\rangle/\partial V = \frac{n}{3}\partial\langle U\rangle/\partial V$, and can be derived from the general thermodynamic relation between the pressure and internal energy, $(\partial\langle U\rangle/\partial V)_T = -P + T(\partial P/\partial T)_V$.

If this relation is rewritten in terms of the Ω_{mn} functions,

$$V\left[\frac{\Omega_{01}(2\Omega_{11}-\Omega_{01}\Omega_{20}) - k_BT\Omega_{11}^2}{1-k_BT\Omega_{20}} - \Omega_{02}\right]$$
$$= -\frac{n}{3}k_BT\left(\frac{\Omega_{11}-\Omega_{01}\Omega_{20}}{1-k_BT\Omega_{20}}\right) + \left(\frac{n}{3}+1\right)\Omega_{01}, \quad \text{(A24)}$$

and uses $\Omega_{11} = C + D\Omega_{20}$ and $\Omega_{02} = A + B\Omega_{20}$, the following expression for Ω_{20} can be derived:

$$\frac{1}{1-k_BT\Omega_{20}} = \frac{\frac{3}{n}P - \frac{3}{n}B_T + D}{k_BTC + D - P}. \quad \text{(A25)}$$

An important identity is $N(k_BTC + D - P) = k_BT\rho n/3$ which allows $\langle K^{-1}\rangle$ or equivalently Ω_{20} and C_V to be obtained only from Z and its first density derivative,

$$\frac{1}{N(1-k_BT\Omega_{20})} = \frac{2}{N(2-k_BT(3N-5)\langle K^{-1}\rangle)}$$
$$= \frac{C_V}{Nk_B} = \frac{3}{2}\left(1-\frac{1}{N}\right) + \frac{3}{n}Z - \frac{9}{n^2}\zeta\frac{\partial Z}{\partial\zeta}. \quad \text{(A26)}$$

The thermodynamic properties of the IP system in terms of $\langle U\rangle$ and its derivative derived within the LTT are summarized in Table I.

[1] J. P. Hansen and I. R. McDonald, *Theory of Simple Liquids*, 3rd ed. (Academic, New York, 2005).
[2] M. Ross, J. Chem. Phys. **71**, 1568 (1979).
[3] J. Dufty and M. H. Ernst, Mol. Phys. **102**, 2123 (2004).
[4] F. de J. Guevara-Rodriguez and M. Medina-Noyola, Phys. Rev. E **68**, 011405 (2003).
[5] A. C. Brańka and D. M. Heyes, Phys. Rev. E **69**, 021202 (2004).
[6] B. B. Laird and D. J. Haymet, J. Chem. Phys. **91**, 3638 (1989).
[7] J. W. Shaner, J. Chem. Phys. **89**, 1616 (1988).
[8] D. Ben-Amotz and G. Stell, J. Chem. Phys. **120**, 4844 (2004).
[9] S. Pyett and W. Richtering, J. Chem. Phys. **122**, 034709 (2005).
[10] S. E. Paulin, B. J. Ackerson, and M. S. Wolfe, J. Colloid Interface Sci. **178**, 251 (1996).
[11] C. N. Likos, A. Lang, M. Watzlawek, and H. Löwen, Phys. Rev. E **63**, 031206 (2001).
[12] B. M. Mladek, G. Kahl, and C. N. Likos, Phys. Rev. Lett. **100**, 028301 (2008).
[13] D. M. Heyes and A. C. Brańka, Soft Matter **5**, 2681 (2009).

[14] C. N. Likos, Phys. Rep. **348**, 267 (2001).
[15] C. N. Likos, Soft Matter **2**, 478 (2006).
[16] F. Ozon, G. Petekidis, and D. Vlassopoulos, Ind. Eng. Chem. Res. **45**, 6946 (2006).
[17] W. G Hoover, S. G. Gray, and K. W. Johnson, J. Chem. Phys. **55**, 1128 (1971).
[18] P. Hutchinson and W. Conkie, Mol. Phys. **24**, 567 (1972).
[19] W. G. Hoover, D. A. Young, and R. Grover, J. Chem. Phys. **56**, 2207 (1972).
[20] L. Verlet and J. J. Weis, Mol. Phys. **24**, 1013 (1972).
[21] L. Verlet and J. J. Weis, Phys. Rev. A **5**, 939 (1972).
[22] D. A. Young and F. J. Rogers, J. Chem. Phys. **81**, 2789 (1984).
[23] D. M. Heyes and A. C. Brańka, Phys. Chem. Chem. Phys. **10**, 4036 (2008).
[24] D. M. Heyes and A. C. Brańka, Mol. Phys. **107**, 309 (2009).
[25] A. C. Brańka, D. M. Heyes, and G. Rickayzen, J. Chem. Phys. **135**, 164507 (2011).
[26] G. Rickayzen, A. C. Brańka, S. Pieprzyk, and D. M. Heyes, J. Chem. Phys. **137**, 094505 (2012).
[27] A. C. Brańka and D. M. Heyes, J. Chem. Phys. **134**, 064115 (2011).
[28] R. Agrawal and D. A. Kofke, Mol. Phys. **85**, 23 (1995).
[29] S. Prestipino, F. Saija, and P. V. Giaquinta, J. Chem. Phys. **123**, 144110 (2005).
[30] R. J. Wheatley, J. Phys. Chem. B **109**, 7463 (2005).
[31] N. S. Barlow, A. J. Schultz, S. J. Weinstein, and D. A. Kofke, J. Chem. Phys. **137**, 204102 (2012).
[32] C. M. Roland, S. Bair, and R. Casalini, J. Chem. Phys. **125**, 124508 (2006).
[33] D. Fragiadakis and C. M. Roland, J. Chem. Phys. **134**, 044504 (2011).
[34] D. Colsovich and C. M. Roland, J. Phys. Chem. B **112**, 1329 (2008).
[35] C. M. Roland, R. B. Bogoslovov, R. Casalini, A. R. Ellis, S. Bair, S. J. Rzoska, K. Czuprynski, and S. Urban, J. Chem. Phys. **128**, 224506 (2008).
[36] U. R. Pedersen, N. P. Bailey, T. B. Schrøder, and J. C. Dyre, Phys. Rev. Lett. **100**, 015701 (2008).
[37] U. R. Pedersen, T. Christensen, T. B. Schrøder, and J. C. Dyre, Phys. Rev. E **77**, 011201 (2008).
[38] N. P. Bailey, U. R. Pedersen, N. Gnan, T. B. Schrøder, and J. C. Dyre, J. Chem. Phys. **129**, 184507 (2008).
[39] N. P. Bailey, U. R. Pedersen, N. Gnan, T. B. Schrøder, and J. C. Dyre, J. Chem. Phys. **129**, 184508 (2008).
[40] T. B. Schrøder, N. P. Bailey, U. R. Pedersen, N. Gnan, and J. C. Dyre, J. Chem. Phys. **131**, 234503 (2009).
[41] N. Gnan, T. B. Schrøder, U. R. Pedersen, N. P. Bailey, and J. C. Dyre, J. Chem. Phys. **131**, 234504 (2009).
[42] T. S. Ingebrigtsen, T. B. Schrøder, and J. C. Dyre, Phys. Rev. X **2**, 011011 (2012).
[43] L. A. Roed, D. Gundermann, J. C. Dyre, and K. Niss, J. Chem. Phys. **139**, 101101 (2013).
[44] M. S. Shell, J. Chem. Phys. **137**, 084503 (2012).
[45] R. Lustig, J. Chem. Phys. **100**, 3048 (1994); **100**, 3060 (1994); **100**, 3068 (1994); **109**, 8816 (1998).
[46] K. Meier and S. Kabelac, J. Chem. Phys. **124**, 064104 (2006).
[47] E. M. Pearson, T. Halicioglu, and W. A. Tiller, Phys. Rev. A **32**, 3030 (1985).
[48] P. Mausbach and R. J. Sadus, J. Chem. Phys. **134**, 114515 (2011).
[49] T. M. Yigzawe and R. J. Sadus, J. Chem. Phys. **138**, 044503 (2013).
[50] J. Mairhofer and R. J. Sadus, J. Chem. Phys. **139**, 154503 (2013).
[51] J. M. Haile, *Molecular Dynamics Simulation: Elementary Methods*, 3rd ed. (Wiley & Sons, New York, 1992).
[52] J. Kolafa, S. Labík, and A. Malijevský, Phys. Chem. Chem. Phys. **6**, 2335 (2004).
[53] T. Boublík and I. Nezbeda, Collect. Czech. Chem. Commun. **51**, 2301 (1986).
[54] T. M. Yigzawe and R. J. Sadus, J. Chem. Phys. **138**, 194502 (2013).
[55] B. C. Freasier, A. Czezowski, and R. J. Bearman, J. Chem. Phys. **101**, 7934 (1994).
[56] N. V. Prabhu and K. A. Sharp, Annu. Rev. Phys. Chem. **56**, 521 (2004).
[57] J. C. Mauro, R. J. Loucks, and S. Sen, J. Chem. Phys. **133**, 164503 (2010).
[58] J. C. Mauro, R. J. Loucks, and S. Sen, J. Chem. Phys. **134**, 147102 (2011).
[59] R. Ladenstein, Biotechnol. Biotechnol. Eq. **22**, 612 (2008).
[60] W. G. Hoover, Phys. Rev. A **34**, 2499 (1986).
[61] See Supplemental Material at http://link.aps.org/supplemental/10.1103/PhysRevE.90.012106 for the soft-sphere system.
[62] D. M. Heyes, S. M. Clarke, and A. C. Brańka, J. Chem. Phys. **131**, 204506 (2009).
[63] Y. Rosenfeld and P. Tarazon, Mol. Phys. **95**, 141 (1998).
[64] J. P. Hansen and L. Verlet, Phys. Rev. **184**, 151 (1969).
[65] H. J. Raveché, R. D. Mountain, and W. B. Streett, J. Chem. Phys. **61**, 1970 (1974).
[66] M. Dijkstra and R. Evans, J. Chem. Phys. **112**, 1449 (2000).
[67] Y. Rosenfeld, Phys. Rev. A **15**, 2545 (1977).
[68] L. Yokoyama, Physica B **254**, 172 (1998).
[69] M. Dzugutov, Nature (London) **381**, 137 (1996).
[70] Y. Rosenfeld, J. Phys.: Condens. Matter **11**, 5415 (1999).
[71] G. X. Li, C. S. Liu, and Z. G. Zhu, Phys. Rev. B **71**, 094209 (2005).
[72] Y. Rosenfeld, E. Nardi, and Z. Zinamon, Phys. Rev. Lett. **75**, 2490 (1995).
[73] J. J. Hoyt, M. Asta, and B. Sadigh, Phys. Rev. Lett. **85**, 594 (2000).
[74] J. R. Errington, T. M. Truskett, and J. Mittal, J. Chem. Phys. **125**, 244502 (2006).
[75] M. Agarwal and Ch. Charkravarty, J. Phys. Chem. B **111**, 13294 (2007).
[76] E. Salcedo, A. B. de Oliveira, N. M. Barraz, Jr., Ch. Charkravarty, and M. C. Barbosa, J. Chem. Phys. **135**, 044517 (2011).
[77] N. H. March and J. A. Alonso, Phys. Rev. E **73**, 032201 (2006).
[78] J. Mittal, J. R. Errington, and T. M. Truskett, Phys. Rev. Lett. **96**, 177804 (2006).
[79] Peng He, Hui Liu, Jiqin Zhu, Yanfeng Li, Shiping Huang, Peng Wang, and Huiping Tian, Chem. Phys. Lett. **535**, 84 (2012).
[80] J. Daligault, Phys. Rev. Lett. **96**, 065003 (2006).
[81] S. Chapman and T. G. Cowling, *The Mathematical Theory of Non-uniform Gases* (Cambridge University Press, Cambridge, UK, 1970).
[82] R. V. Vaz, A. L. Magalhães, D. L. A. Fernandes, and C. M. Silva, Chem. Eng. Sci. **79**, 153 (2012).

[83] Qi-Long Cao, Xiang-Shan Kong, Y. D. Li, Xuebang Wu, and C. S. Liu, Physica B **406**, 3114 (2011).
[84] Y. D. Fomin, V. N. Ryzhov, and N. V. Gribova, Phys. Rev. E **81**, 061201 (2010).
[85] E. G. D. Cohen and L. Rondoni, Phys. Rev. Lett. **84**, 394 (2000).
[86] J. L. Bretonnet, J. Chem. Phys. **117**, 9370 (2002).
[87] A. Samanta, Sk. Musharaf Ali, and S. K. Ghosh, Phys. Rev. Lett. **92**, 145901 (2004).
[88] S. Bastea, Phys. Rev. Lett. **93**, 199603 (2004).
[89] S. Bastea, J. Chem. Phys. **135**, 084515 (2011).
[90] W. P. Krekelberg, M. J. Pond, G. Goel, V. K. Shen, J. R. Errington, and T. M. Truskett, Phys. Rev. E **80**, 061205 (2009).
[91] C. De Michele, F. Sciortini, and A. Coniglio, J. Phys.: Condens. Matter **16**, L489 (2004).
[92] S. Bair, Tribol. Trans. **43**, 91 (2000).
[93] S. Bair, J. Jarzynski, and W. O. Winer, Tribol. Int. **34**, 461 (2001).
[94] R. Casalini and S. Bair, J. Chem. Phys. **128**, 084511 (2008).
[95] V. V. Kechin, J. Phys.: Condens. Matter **16**, L125 (2004).
[96] F. D. Stacey, J. Phys.: Condens. Matter **11**, 575 (1999).